Monte Carlo Simulations of Ag^+ and Ag in Aqueous Solution. Redox Potential of the Ag^+/Ag Couple

Vincent Dubois, Pierre Archirel,* and Anne Boutin

Laboratoire de Chimie-Physique, UMR 8000, Bât. 350, Université Paris-Sud, 91405 Orsay Cédex, France

Received: December 31, 2000; In Final Form: March 21, 2001

We have performed Monte Carlo simulations of the Ag^+ cation and of the Ag atom in water. We have used the Kozack and Jordan polarizable water potential. The pairwise solute−water potentials and the three-body cation−water potential are based on MP2 calculations. We get for the hydration enthalpy of Ag^+ the value -5.65 ± 0.15 eV, in good agreement with the experimental value: -5.5 ± 0.1 eV. For the ionization free energy of Ag, we have tested three available methods (thermodynamic perturbation, overlapping distribution, and self-consistent histograms methods) and found out that they yield very close results. The redox potential of the Ag^+/Ag couple is estimated to be −2.3 V/NHE. Since our potentials include no empirical data, the agreement with the electrochemical value, −1.9 V/NHE, and the thermochemical value, −2.1 V/NHE, is satisfactory.

1. Introduction

The physical chemistry of silver cations, atoms, and clusters in solution is now very well documented,[1] in particular absorption spectra of small transient species have been recorded[2] and redox potentials of the bare and liganded couples Ag^0L_2/Ag^+L_2 have been evaluated.[3,4] In contrast theoretical investigations of this field have been scarce. A few years ago we could give an estimation of the above-mentioned redox potentials,[3,4] but with an oversimplified method. In the present article we present Monte Carlo calculations of the hydration enthalpy of Ag^+ and Ag and of the redox potential of the couple Ag^+/Ag.

The Monte Carlo method has been widely used for the calculation of hydration enthalpies of metal cations: among others, simulations of the solvation of Li^+ and Na^+,[5] Mg^{2+} and Ca^{2+},[6] Cu^{2+},[7] and Cr^{3+} [8] have been reported. The method, coupled to *thermodynamic perturbation*,[9,10] has also been applied to the calculation of hydration *differential* free energies, for example, between Li^+ and Na^+.[5,11] To our knowledge no attempt has been made of evaluating absolute ionization energies of metal atoms in solution with thermodynamic perturbation.

In the second section of this article, we give the different contributions to the interaction energy, used in the Monte Carlo simulations. In the third section we discuss the experimental values of the solvation enthalpy and redox potential. In the fourth section we discuss the results of the Ag^+ and Ag simulations, and in the fifth section the value of the redox potential.

2. Calculation of the Energy

We have used the usual decomposition of the interaction energy into solvent−solvent, polarization, pairwise, and three-body solute−solvent contributions, according to the following formulas:

$$E_{\text{int}}^0 = E_{\text{water}} + E_{\text{pol}} + E_{\text{solute-water}}^{\text{pair}} \tag{1}$$

$$E_{\text{int}} = E_{\text{int}}^0 + E_{\text{Ag(H}_2\text{O)}_n}^{3-\text{body}+} \tag{2}$$

These four contributions are discussed in the following subsections:

2.1. Water Potential. We have chosen the rigid water potential of Kozack and Jordan,[12] hereafter referred to as KJ. Within this potential the water molecule is modeled with four sites: the three O and H atoms and an additional "δ" site, located inside the H_2O molecule, on the symmetry axis. These four sites bear electric point charges and the δ site is also used as unique center for isotropic Lennard-Jones (LJ) interaction and for polarization. The charges have been calculated so as to reproduce the first multipoles of isolated H_2O and the LJ parameters optimized so as to reproduce the second virial parameter $B(T)$ of water steam.

With this potential the authors could well reproduce the structure and energetics of small water clusters, and also rather well radial distribution functions (RDF) in the liquid phase. On the other hand the mean interaction energy and density in the liquid phase are only in qualitative agreement with experimental values: −0.5 eV (experimental, −0.43 eV) and 1.038 g/cm^3 (experimental, 1.0 g/cm^3), respectively.

We have thus also performed a few tests with the PSPC potential.[13] This potential is a polarizable potential of the same type as KJ, but with the LJ and polarization sites located on the O atom. The values of the PSPC parameters have been adjusted for reproducing properties of bulk liquid water, with no particular concern about water clusters. This potential actually proved less efficient than KJ for the description of solvation. This point will be developed in section 2.5.

2.2. Polarization of the Solvent. Self-polarization of the solvent and its polarization by the solute are important and non additive phenomena. In addition, one can expect that the cation in solution not only polarizes the solvent, but also modifies the self-polarization of the solvent. It is thus necessary to calculate the polarization energy explicitly. In the KJ approach, polarization of H_2O is assumed to be isotropic, this implies that we use only one polarization site (δ) and the mean value of the dipole

* Corresponding author. E-mail: pierre.archirel@lcp.u-psud.fr. Fax: 33 1 69 15 61 88.

10.1021/jp0045888 CCC: $20.00
Published on Web 08/28/2001

polarizabilty α of H_2O (1.47 Å^3).[12] The polarization energy is calculated in the simplest classical way, formerly proposed by Vesely:[14]

$$E_{\text{pol}} = -\frac{1}{2}\alpha \sum_i \vec{E}_{0i}\vec{E}_i \tag{3}$$

where $\vec{E}_{0i}$ is the electric field on the ith site, due to all the permanent charges, and $\vec{E}_i$ is due to the permanent charges and induced dipoles. The total fields $\vec{E}_i$ must be calculated iteratively. We have used the convergence criterion of Vesely:[14]

$$\frac{\sum_i |\vec{E}_i(n) - \vec{E}_i(n-1)|^2}{\sum_i E_i^2(n)} < 10^{-4} \tag{4}$$

where n is the iteration step.

2.3. Ag^+-H_2O Pairwise Potential. To our knowledge no Ag^+-H_2O potential is available in the literature. We thus have built such a potential, and chosen to use ab initio data on the cluster Ag^+H_2O. According to formula 1, the cation−water potential excludes the polarization interaction, it thus must reproduce the difference between the two following energies: the ab initio interaction energy of the Ag^+H_2O cluster and the polarization energy of the same cluster, using formula 3

We have chosen the MP2 ab initio level[15,16] (with no BSSE correction; for H_2O we have used the basis set of ref 18 and for Ag the core pseudopotential and basis set of ref 29), because at this level the binding energy of Ag^+H_2O amounts to 1.47 eV, in close agreement with the measured value: 1.4 ± 0.1 eV.[17] We have used the MP2 energies of a few hundred configurations for fitting the parameters of the potential, according to

$$E^{\text{pair}}_{Ag^+-\text{water}} = E^{\text{elec.}}_{Ag^+-\text{water}} + E^{\text{disp.rep.}}_{Ag^+-\text{water}} \tag{5}$$

with

$$E^{\text{elec.}}_{Ag^+-\text{water}} = \sum_S \frac{q_S}{R_S} \tag{6}$$

and

$$E^{\text{disp.rep.}}_{Ag^+-\text{water}} = \sum_S \left(\sum_{n=3,4,6} \frac{A_{S,n}}{(R_S)^n} + \frac{A_{S,20}}{(R_S)^{20}} + C_S e^{-\beta_S R_S} \right) \tag{7}$$

In these formulas, R_S is the distance from Ag^+ to site S. These S sites are the three atoms O and H (with HOH = 105.55° and d_{OH} = 0.9713 Å), and two additional γ sites. The linear parameters of the potential: q, A, and C have been optimized by a least-squares procedure. The nonlinear parameter β has been optimized on a grid, as well as the values of three exponents n, between 3 and 12 (optimal values: 3, 4, and 6). An additionnal term in R^{-20} has been imposed because it proved efficient. The position of the γ sites has also been optimized (in the H_2O plane): we have found that the optimal position is on the midpoints of the OH bonds. We have found that the quality of the fit is hardly affected by the value of the charge on O, so that we could set it to 0, with no loss of accuracy. The values of the parameters are given in Table 1. The RRMS of the fit amounts to 2%.

2.4. Ag^+-H_2O Three-Body Potential. Calculating the interaction energy with eq 1 yields a poor description of the $Ag^+(H_2O)_n$ clusters, due to the nonadditivity of exchange contributions: for example, the binding energy of the $Ag^+(H_2O)_6$ cluster is found to be ca. 0.5 eV too large. We have introduced the nonadditivity correction in the first solvation shell only, and since the simulation shows that the coordination number of the cation is close to six, we have evaluated this correction for the cluster $Ag^+(H_2O)_6$ only, so that formula 2 now reads:

$$E_{\text{int}} = E^0_{\text{int}} + E^{\text{3-body}}_{Ag^+(H_2O)_6} \tag{8}$$

Since the MP2 investigation of this cluster is very time-consuming, we have worked in two steps, investigating first the potential surface of $Ag^+(H_2O)_2$ extensively, and then that of $Ag^+(H_2O)_6$ more rapidly. We thus have first calculated the difference between E^0_{int} (eq 1) and the MP2 interaction energies for a hundred of geometries of the $Ag^+(H_2O)_2$ system. Note that this energy difference not only includes the exchange nonadditivity, but also the errors due to the use of the KJ water potential and of the classical polarization:

$$E_{\text{MP2}} - E^0_{\text{int}} = E_{\text{exch}} + \delta E_{\text{KJ}} + \delta E_{\text{pol}} \tag{9}$$

This difference has been represented through the following analytic form:

$$E^{\text{3-body}}(\text{Ag}\delta_1\delta_2) = Ae^{-aR_{\text{Ag}\delta_1}}e^{-aR_{\text{Ag}\delta_2}}e^{-bR_{\delta_1\delta_2}} \tag{10}$$

where δ_i is the KJ δ additional site of the ith water molecule (section 2.1). We now postulate that the nonadditive potential for the $Ag^+(H_2O)_6$ system is given by the simple formula:

$$E^{\text{3-body}}_{Ag^+(H_2O)_6} = \lambda \sum_{i<j=1,6} E^{\text{3-body}}(\text{Ag}\delta_i\delta_j) \tag{11}$$

We have optimized λ, so as to reproduce the MP2 energies of a list of 10 $Ag^+(H_2O)_6$ clusters. The values of the parameters of formulas 10 and 11 are given in Table 1. We emphasize that the present value of the λ parameter is closely related to the $Ag^+(H_2O)_6$ cluster, and can give a poor description of the other clusters $Ag^+(H_2O)_n$, with $n \leq 5$.

2.5. Comparison of the KJ and PSPC Water Potentials. As already mentioned we have also tried to use the PSPC water potential, and consequently to build the corresponding cation−water pairwise and three-body potentials. We have succeeded in building the pairwise potential, but not the three-body potential, because using PSPC made the reproduction of the MP2 binding energy of the cluster $Ag^+(H_2O)_2$ impossible. Actually the functional form of eq 10 can only represent contributions which always have the same sign, like the

TABLE 1: Parameters of the Pairwise and Three-Body Ag^+-H_2O Potentials, According to Equations 6, 7, 10, and 11

parameter	value (au)	parameter	value (au)
q_O	0.0	C_O	−21602.65
q_H	0.692	C_H	22.993
q_γ	−0.692	C_γ	−3.505
A_{O3}	24.621	β_O	4.0
A_{O4}	−140.006	β_H	2.0
A_{O6}	835.788	β_γ	1.1
A_{O20}	34 737 622.6		
A_{H3}	6.496	A	7.785
A_{H4}	−28.008	a	0.429
A_{H6}	40.611	b	0.582
A_{H20}	−1 327.29	λ	0.5
$A_{\gamma 3}$	−18.289		
$A_{\gamma 4}$	86.754		
$A_{\gamma 6}$	−194.109		
$A_{\gamma 20}$	1 703 114.38		

TABLE 2: Parameters of the Pairwise Ag−H_2O Potential, According to Equation7

parameter	value (au)	parameter	value (au)
A_{O10}	378 811.16	C_O	−72 729 245.9
A_{O11}	−2 222 688.91	C_H	429.832 67
A_{O16}	1 117 743 220.0	C_γ	−72 463.710 7
A_{O20}	−25 979 429 100.0		
A_{H10}	−15 843.794 6	β_O	5.2
A_{H11}	33 088.044 2	β_H	2.8
A_{H16}	−174 954.312	β_γ	3.8
A_{H20}	614 143.36		
$A_{\gamma 10}$	−83 992.271 1		
$A_{\gamma 11}$	461 452.24		
$A_{\gamma 16}$	−16 152 266.6		
$A_{\gamma 20}$	172 038 566.0		

exchange nonadditivity (term 1 of eq 9), and not contributions with changing signs (terms 2 and 3 of eq 9). In the PSPC case these last terms usually dominate, making the fit of the parameters of formula 10 impossible. With the KJ potential this fit is possible, because the terms 2 and 3 are always small.

This shows that the KJ potential describes the interactions between water molecules in the first solvation shell, better than PSPC. This is due to the fact that the authors of KJ have built their potential exclusively from gas-phase data, thus including information about large parts of the potential surface of the water dimer, unlike PSPC, optimized for bulk water.

2.6. Ag−H_2O Pairwise Potential. We have built a pairwise Ag−H_2O potential of the form given by eq 7. The parameters of this potential have been determined with the help of the MP2 potential surface of Ag H_2O, but since accurate calculations show that the AgH_2O interaction is very weak (0.02 eV[18]), we have considered that every attractive interaction energy is due to BSSE (basis set superposition error) and set it to zero. For the same reason we have introduced no polarization of the Ag atom and no specific three-body interaction. For Ag we thus use eq 1 only. The parameters of the potential are given in Table 2.

3. About "Experimental" Values of Redox Potentials and Hydration Enthalpies

3.1. Electrochemical Value of the Redox Potential of the Ag^+/Ag Couple. The direct evaluation of this redox potential has not been made; however, it is possible to deduce its value from the value of the electrode potential of the silver electrode, which is known with a great accuracy: 0.7996 V/NHE.[19] Indeed, this electrode potential is the redox potential of the Ag^+/Ag_{solid} couple, and can be related to the redox potential of the Ag^+/Ag couple with the help of the following thermodynamic cycle:[20]

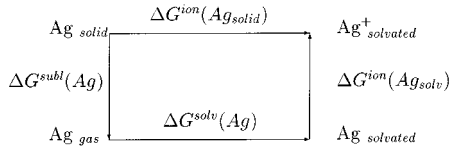

This cycle has been written with free enthalpies, because the potential (redox potential or electrode potential) is related to the ionization free enthalpy (of atomic or solid Ag, respectively) through the following equation:

$$E°(M^+/M) = \Delta G^{ion}(M)/|e| + ENHE \qquad (12)$$

where the free enthalpy is given in eV, the potential in V/NHE (volts relative to the normal hydrogen electrode), and $|e| = 1$ is the elementary charge. ENHE is the absolute potential of the standard hydrogen electrode. The value −4.43 V is currently used, with an error bar of 0.05 eV.[21] From the thermodynamic cycle and eq 12 we can write the following relationship:

$$E°(Ag^+/Ag) = E°(Ag^+/Ag_{solid}) - \Delta G^{solv}(Ag) - \Delta G^{subl}(Ag) \qquad (13)$$

We now examine the two required quantities of this equation: the sublimation free enthalpy of solid silver amounts to +2.55 eV.[19] This number is given without error bar. The hydration free enthalpy of atomic silver amounts to +0.15 ± 0.1 eV. The evaluation of this quantity will be detailed in section 4.3. We now get for the redox potential of the Ag^+/Ag couple the "measured" electrochemical value −1.9 eV.

3.2. Thermochemical Values. Hydration enthalpies of individual ions are not directly measurable, and must be deduced from a set of data for anion−cation pairs. The published data is thus usually given on a relative scale, with either the formation enthalpy of proton in solution: see Krestov,[22] or for the hydration enthalpy of the proton, see Burgess,[23] taken as zero. Since these two reference quantities differ by a well-known quantity, i.e., the gas phase formation enthalpy of proton, 15.91 eV,[24] we can compare the values given by these two authors: +6.37 eV (Burgess) and +6.47 eV (Krestov), relative to the hydration enthalpy of proton. It can be seen that these two values agree within 0.1 eV: in our discussions we shall use the average value +6.40 eV.

The accurate evaluation of the hydration enthalpy of proton in solution proved difficult, and several values have been proposed. Krestov and Burgess used the value −11.3 eV, which yields for the hydration enthalpy of Ag^+ the absolute value −4.9 eV. This hydration enthalpy of proton has been recently revisited, and the accurate value −11.91 ± 0.01 eV proposed.[24] This last value enables an update of the absolute value of the Ag^+ hydration enthalpy: we now obtain −5.5 ± 0.1 eV, which we will use in our discussions.

It is possible to deduce a thermochemical value of the redox potential of the Ag^+/Ag couple from this hydration enthalpy of Ag^+. For this purpose we have used the thermodynamic cycle:

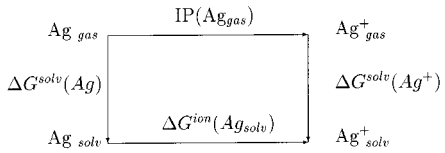

according to which

$$\Delta G^{ion}(Ag_{solv}) = IP(Ag_{gas}) + \Delta H^{solv}(Ag^+) - T\Delta S^{solv}(Ag^+) - \Delta G^{solv}(Ag) \qquad (14)$$

We have used the measured values of $IP(Ag_{gas})$, gas-phase ionization potential of atomic silver, 7.58 eV,[19] and of $\Delta H^{solv}(Ag^+)$, hydration enthalpy of Ag^+, −5.5 eV. We have also used our estimated value of $\Delta G^{solv}(Ag)$, hydration free enthalpy of neutral Ag, +0.15 eV (section 4.3). We have also obtained the value of $T\Delta S^{solv}(Ag^+)$, hydration entropy of Ag^+, from different experimental data,[23,24] and found the value −0.4 eV.

Using eq 12 and 14 we now get the value −2.1 V/NHE for the redox potential of the Ag^+/Ag couple. This value agrees with the electrochemical value: −1.9 V/NHE within 10%. Since both values have been deduced from several contributions, some of which suffer from significant uncertainties, we shall not

decide which one is the most reliable, and shall compare our results to the two values.

4. Hydration Enthalpy and Radial Distribution Functions for Ag^+ and Ag

4.1. Conditions of the Ag^+ Simulations. We have used the Monte Carlo method, with a simulation box containing 275 water molecules, with and without one Ag^+ cation, at 298 K. Since an NPT simulation of pure KJ water yields a value of the density which is too large (1.055 g/cm^3, in agreement with the result of ref 12), we have preferred to perform NVT simulations. For pure water the value of the volume has been calculated, so as to yield a value of this density equal to 1. g/cm^3. For solvated Ag^+ we have used the same volume value: this is justified by the fact that in the NPT simulation, solvation of Ag^+ induces only an extremely small variation of volume (-1 Å^3). This is also justified by the fact that the measured values of this volume variation for Li^+ and Na^+ are very small ($-11.$ Å^3 [5]).

We have used periodic boundary conditions, and the same value (9 Å) for the cutoff radius of the three contributions to the interaction energy: KJ potential, pairwise Ag^+H_2O potential and polarization. Concerning electrostatic long range correction, we used a reaction field and the experimental value of the dielectric constant of water ($\epsilon = 78$[19]).

We have used the Metropolis algorithm,[25] with an acceptance ratio of 45%. This ratio is yielded by the following values of the maximum displacements: 0.13 Å and 15° (displacement and rotation of H_2O), 0.1 Å (displacement of Ag^+). We have used preferential sampling,[26] which multiplies the number of attempted moves in the vicinity of the solute by a factor two. This is achieved by the following law:

$$P(i) = \frac{1}{R_i^2 + 75.} \qquad (15)$$

where $P(i)$ is the probability of sampling the ith molecule and R_i its distance (in angstroms) to the solute. We have adjusted the sampling probability of the solute, so as to make it close to the probability of sampling water in the first solvation shell.

4.2. Results for Ag^+. The hydration enthalpy of Ag^+ is well approximated by the difference of the two average energies:

$$\Delta H_{solv}(Ag^+) = \langle E_{int}(Ag^+(H_2O)_n)\rangle - \langle E_{int}(H_2O)_n\rangle \quad (16)$$

Two simulations with 80×10^6 MC steps have given the value -5.65 ± 0.15 eV of the solvation enthalpy. The error bar is estimated from the results for two blocks of 40×10^6 MC steps each. It can be seen that this result is very close to the measured value -5.5 ± 0.1 eV, and that the error bars even overlap. The contributions of the polarization and three-body effects amount to -1.0 and $+0.4$ eV, respectively.

The Ag^+-O and Ag^+-H radial distribution functions (RDF) are shown in Figure 1. They are qualitatively comparable to those obtained for similar cations.[5] Two solvation shells are visible, but only the first one is well structured, with a maximum value at $R_{AgO} = 2.3$ Å. The result of the integration of the Ag^+-O RDF is shown on the same figure. It can be seen that the RDF never vanishes, and that consequently the integrated value has no plateau: this means that the coordination number is not well-defined. Stopping the integration at $R_{AgO} = 2.85$ Å (approximate end of the first peak) yields the value 6 for this number, but we have checked from snapshots of the simulation that a number between 6 and 7 is also plausible. This number is larger than that obtained for other singly charged cations, such as Li^+(value: 4) and Na^+ (value: 5−6),[5] in normal correlation with increasing size of the cation.

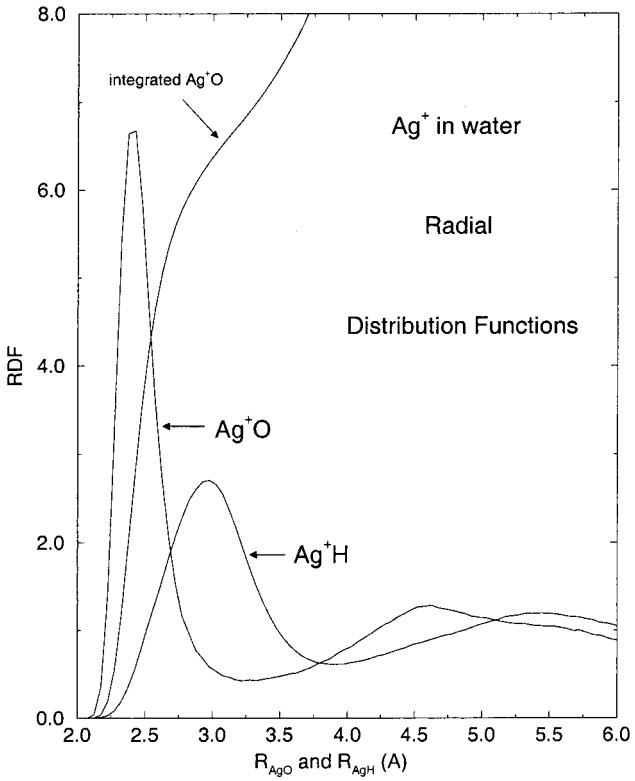

Figure 1. Ag^+-O and Ag^+-H radial distribution functions from a Monte Carlo NVT simulation of Ag^+ in aqueous solution.

4.3. Results for Ag. For the Ag atom, we have used the same simulation conditions as for Ag^+; only the cutoff value of the $Ag-H_2O$ potential has been set to 3 Å. We obtain for the hydration enthalpy the value $+0.05 \pm 0.1$ eV: this number is very small, as expected for a neutral solute with no permanent moments.

The Ag−O and Ag−H RDF are shown in Figure 2. These RDF are much less structured than that of Ag^+, nevertheless two solvation shells are visible, so that we can expect an entropic effect. For evaluating this effect we have used the theoretical study of Lynden-Bell et al.,[27] about the hydration entropy of spherical neutrals, and its variation toward the size of the solute. Estimating the value of the cavity radius of Ag from the AgO RDF to be 2.5 Å, we get for the entropic effect the value $T\Delta S^{solv} = -0.1 \pm 0.05$ eV. This yields for the hydration free enthalpy of the Ag atom the value $+0.15$ eV: this value has been used in the evaluation of the "experimental" values in section 3.

The hydration free enthalpy of atomic Ag is thus small but clearly hydrophobic. The leading effect may be called "cavitation entropy": the metal atom excludes water from its volume, this results in a reorganization of the hydrogen-bond network of water. This value can be compared to the available measured value for the mercury atom: $+0.08$ eV,[28] which is close to that for the silver atom, within the uncertainties. Since the leading phenomenon is a cavitation, we understand that the value for mercury is smaller, due to the smaller size of this atom.

5. Redox Potential of the Ag^+/Ag Couple

5.1. Methods. We will consider that the ionization free enthalpy is well approximated by the ionization NVT *free energy* ΔF^{ion}: this is justified by the fact already mentioned that the solvation of Ag^+ induces almost no variation of volume. The

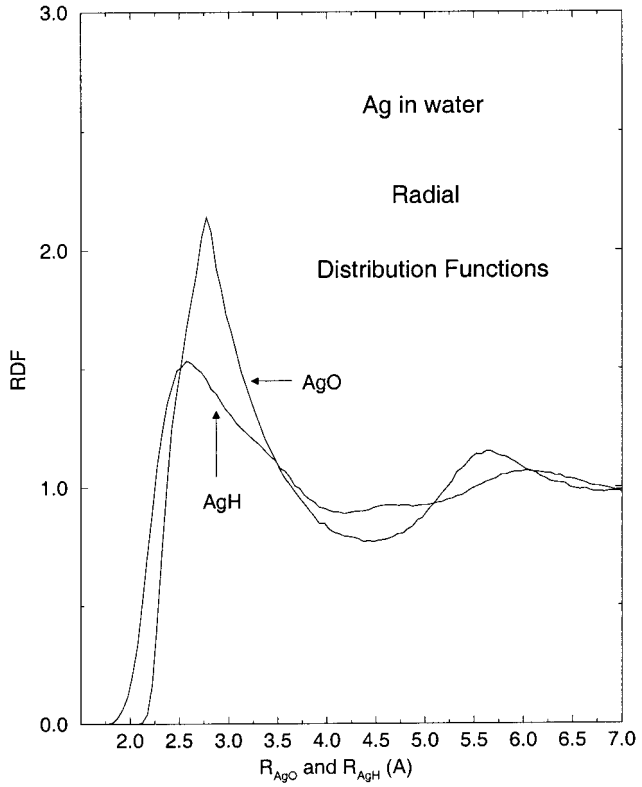

Figure 2. Ag−O and Ag−H radial distribution functions from a Monte Carlo NVT simulation of Ag in aqueous solution.

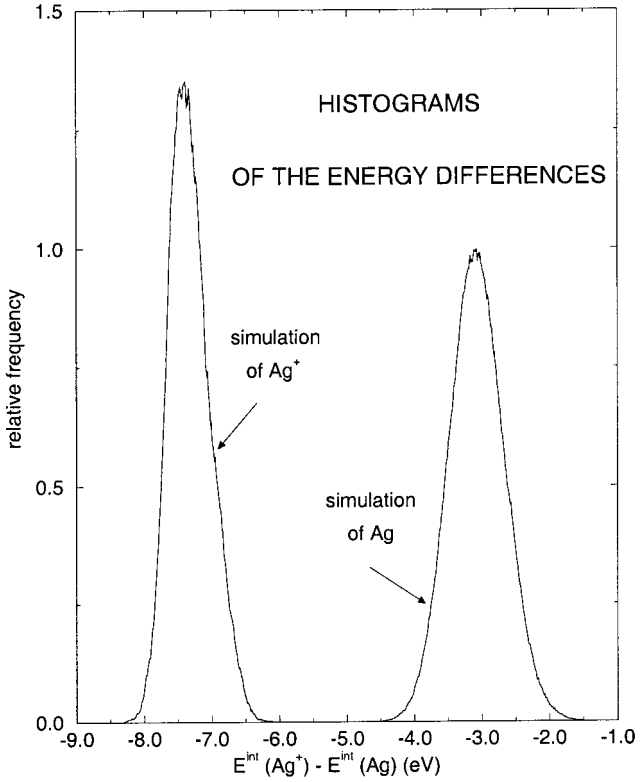

Figure 3. Histograms of the energy differences in the NVT simulations of Ag^+ and Ag.

ionization free energy is given by

$$\Delta F^{\text{ion}}(\text{Ag}) = \Delta F^{0\rightarrow 1} + \text{IP}(\text{Ag}_{\text{gas}}) \tag{17}$$

where $\Delta F^{0\rightarrow 1}$ is the free energy of the $Ag \rightarrow Ag^+$ mutation. We call mutation the simple change of the solute−water potential (from that of Ag to that of Ag^+), assuming that both species Ag and Ag^+ have no internal energies. $IP(Ag_{gas})$ amounts to 7.58 eV (section 3.2).

For the calculation of the mutation free energy we have used three methods, described in the literature:[9,10] the thermodynamic perturbation (TP), the overlapping distribution (OD), and the self-consistent histograms (SCH).

Within the TP method, the mutation free energy can be calculated through adding up contributions of intermediate states characterized by $\lambda_i = id\lambda$, according to:

$$\Delta F^{0\rightarrow 1} = -kT \sum_{i=0}^{9} \ln\langle e^{-(E^{\lambda_{i+1}} - E^{\lambda_i})/kT} \rangle_{\lambda_i} \tag{18}$$

$$E^{\lambda_i} = (1 - \lambda_i) E_{\text{int}}(\text{Ag}) + \lambda_i E_{\text{int}}(\text{Ag}^+) \tag{19}$$

The bracket $\langle\ \rangle_{\lambda_i}$ means that the mean value is calculated in a simulation with a potential given by eqs 2 and 19. We have considered 10 values of λ_i and both the *forward* simulation, with $d\lambda = 0.1$, yielding $\Delta F^{0\rightarrow 1}$, and the *backward* simulation, with $d\lambda = -0.1$, yielding $\Delta F^{1\rightarrow 0}$. These two mutation free energies were calculated in the same run. The thermodynamic perturbation method requires the averaging of the exponential of eq 18, and thus must be used carefully in the present case, because the Ag^+-H_2O and $Ag-H_2O$ potentials are very different. We have decided to work with 10 intermediate potentials only, but with long simulations: 10×10^6 MC steps for each value of λ_i.

The overlapping distribution method requires only two simulations for Ag and Ag^+: for each of these simulations we draw the histogram of the following quantity:

$$\Delta U = E_{\text{int}}(\text{Ag}^+) - E_{\text{int}}(\text{Ag}) \tag{20}$$

If these two histograms overlap, ΔF can be extracted with a very simple manipulation.[9] However, it can be seen in Figure 3 that in the present case the two histograms do not overlap at all; we thus have used the two following possibilities, proposed in ref 9: (i) simple extrapolation of the two histograms by a common fit, giving an estimation of the result, and (ii) use of the more sophisticated SCH method. In this case several simulations are performed with the intermediate potentials of eq 19, and for each of these simulations the histogram of the quantity ΔU of eq 20 is drawn. ΔF is then given by an iterative process.

5.2. Results and Discussion. *5.2.1. Values of the Redox Potential, Entropic Contribution.* The ionization free energy of Ag and the redox potential of the Ag^+/Ag couple, given by the three methods are shown in Table 3. We first discuss the results given by the three methods: (i) The TP method yields forward and backward results which are almost equal, in addition this result is almost equal to the SCH result. This shows that the TP method is quite reliable for the calculation of ionization energies, provided the convergence of the statistics is carefully checked. (ii) We have found that the convergence of the ΔU histograms is much faster than that of the average value of the exponential of eq 18. We thus think that SCH is more convenient that TP. (iii) The simple common fit method gives a result which is only slightly different. This result encourages the use of the common fit method, which is much faster than the two other ones.

We thus consider that the accurate calculated value is −2.3 V/NHE. This value is more negative than the two measured

TABLE 3: Ionization Free Energy of Ag in Water and Entropic Contribution (in eV) and Redox Potential of the Couple Ag^+Ag(in V/NHE)

method	ΔF^{ion}	$T\Delta S^{ion}$	redox potential
TP forward	2.10	−0.22	−2.3
TP backward	2.08	−0.20	−2.3
SC histograms	2.10	−0.22	−2.3
overlapping distribution	2.19	−0.31	−2.2
exptl[a]			−1.9
exptl[b]			−2.1

[a] Experimental value deduced from electrochemical data, see section 3.1. [b] Experimental value deduced from thermochemical data, see section 3.2.

values. It differs from the electrochemical value by 20%, and from the thermochemical value by 10% only. Since our value has been obtained with an ab initio strategy, i.e., with no parameter adjustment, we consider that our result is in good agreement with experiments.

The ionization entropy has been calculated with the following formula:

$$T\Delta S^{ion} = -\Delta F^{0\rightarrow 1} + \Delta H^{solv}(Ag^+) - \Delta H^{solv}(Ag) \quad (21)$$

It can be seen in Table 3 that the entropy contribution is negative and relatively small: −0.2 eV and contributes only 10% to the ionization free energy. Since the corresponding experimental value is not available, we now rather discuss the solvation entropy of Ag^+, for which the experimental value is available: $T\Delta S = -0.4$ eV (section 3.2).

Using our calculated entropy for Ag ionization ($T\Delta S = -0.2$ eV) and the published entropy for Ag hydration ($T\Delta S = -0.1$ eV, section 4.3), we obtain for the Ag^+ solvation the value −0.3 eV. The measured value is thus more negative than our by 30%. Since the value of the hydration entropy of Ag also suffers from uncertainty, this conclusion is fragile, however.

5.2.2. Discussion of the Potentials. We now discuss the separate errors on the enthalpy and entropy of Ag^+ solvation, in connection with the potentials which we have used. This discussion is possible if one considers the thermochemical values only, because our error can then be split into the two contributions: (i) the error on the enthalpy, −0.1 eV (section 4.2) corresponds to a good precision of 2.%. We conclude that our cation−water potentials are reliable. (ii) the error on the entropic effect amounts to −0.1 eV also (section 5.2.1), but corresponds to a large relative error of 30%. The ordering of the water molecule around the solute is determined by the relative intensities of the solute−water and water−water potentials. Now we know first that our cation−water potential is reliable, and second that the KJ potential is too attractive: see section 2.1. The hypothesis that our simulations underestimate the entropic effect is thus plausible.

6. Conclusion

In this work we have performed NVT Monte Carlo simulations of Ag^+ and Ag in aqueous solution at 298 K. We have used the water potential of Kozack and Jordan,[12] the classical polarization method of Vesely,[14] a pairwise and three-body potential for the Ag^+-H_2O interaction, and a pairwise potential for $Ag-H_2O$. The Ag^+-H_2O potentials are analytic representations of MP2 ab initio results, obtained for a series of isolated Ag^+H_2O, $Ag^+(H_2O)_2$ and $Ag^+(H_2O)_6$ clusters. The $Ag-H_2O$ potential is deduced from MP2 ab initio energies of the AgH_2O cluster. Our value of the hydration enthalpy of Ag^+, −5.65 eV, is very close to the measured value, −5.5 eV. This shows that our Ag^+-H_2O potentials are reliable. The Ag^+-O and Ag^+-H radial distribution functions display a clear first solvation shell, and also a second shell. The coordination number of Ag^+ is estimated to be 6, but is probably a little bit larger.

We have also performed a simulation of neutral Ag in water. The hydration enthalpy of Ag amounts to $+0.05 \pm 0.1$ eV. The RDF show that the water molecules are ordered in two solvation shells, an entropy effect is thus to be expected.

We have finally calculated the redox potential of the Ag^+/Ag couple, and compared three different methods. We have found that the Thermodynamic Perturbation method is usable, despite the fact that the Ag^+-H_2O and $Ag-H_2O$ potentials are very different, provided precautions are taken. The simulation of the $Ag \rightarrow Ag^+$ mutation proved accurate enough with 10 intermediate potentials, and with several millions MC steps for each of them. This requirement makes the perturbation method very time-consuming, however the same result can be obtained with the much faster self-consistent histogram method, and a good estimation of the result is also given by the still faster overlap distribution method, including the common fit technique.

Our accurate value of the redox potential is −2.3V/NHE, slightly more negative than the experimental values: −1.9V/NHE (electrochemical value) and −2.1V/NHE (thermochemical value). Since we have used no experimental data for building our potential, we consider that our result is in reasonable agreement with the measured values.

The present results show that the KJ potential is well adapted to our ab initio strategy. The KJ description of the first solvation shell is realistic, and the residual error can be corrected by the additional "three-body" potential. If we now consider bulk water, KJ is known to be too attractive. This feature has different consequences as for enthalpy and entropy: (i) the value of the hydration enthalpy is hardly affected, because the KJ error is almost the same for bulk water and for hydrated Ag^+; (ii) conversely, this error is suspected to lead to an underestimation of the entropy contribution to Ag^+ solvation free energy.

Finally we can expect that, despite the residual error, *differential* effects will be well reproduced, for instance the variation of the redox potential when ligands are added, and when silver aggregation is performed. Work in this direction is in progress.

Acknowledgment. We thank IDRIS (Institut pour le Développement et les Ressources en Informatique Scientifique) for an allocation of computer time, Project 1327. We also thank J. Belloni and M. Mostafavi for fruitful discussions.

References and Notes

(1) Belloni, J.; Mostafavi, M. In *Metal Clusters in Chemistry*; Braunstein, P., Oro, L. A., Raithy, P. R., Eds.; Wiley: New York, 1999; p 1213.
(2) Ershov, B. G.; Janata, E.; Henglein, A.; Fojtik, A. *J. Phys. Chem.* **1993**, *97*, 4589.
(3) Rémita, S.; Archirel, P.; Mostafavi, M. *J. Phys. Chem.* **1995**, *99*, 13198.
(4) Texier, I.; Rémita, S.; Archirel, P.; Mostafavi, M. *J. Phys. Chem.* **1996**, *100*, 12472.
(5) Cieplak, P.; Kollman, P. *J. Chem. Phys.* **1990**, *92*, 6761.
(6) Bernal-Uruchurtu, A. I.; Ortega-Blake, I. *J. Chem. Phys.* **1995**, *103*, 1588.
(7) Pranowo, H. D.; Rode, B. M. *J. Chem. Phys.* **2000**, *112*, 4212.
(8) Martinez, J. M.; Hernandez-Cobos, J.; Saint-Martin, H.; Rappalardo, R. R.; Ortega-Blake, I.; Sanchez-Marcos, E. *J. Chem. Phys.* **2000**, *112*, 2339.
(9) Frenkel, D.; Smit, B. *Understanding Molecular Simulation*; Academic Press: New York, 1996.
(10) Kollman, P. *Chem. Rev.* **1993**, *93*, 2395.
(11) Kim, H. S. *Chem. Phys.* **2000**, *253*, 305.
(12) Kozack, R. E.; Jordan, P. C. *J. Chem. Phys.* **1992**, *96*, 3120.

(13) Engström, S.; Ahlström, P.; Wallqvist, A.; Jönsson, B. *Mol. Phys.* **1989**, *68*, 563.
(14) Vesely, F. J. *J. Comput. Phys.* **1977**, *24*, 361.
(15) Frisch, M. J.; Trucks, G. W.; Schlegel, H. B.; Scuseria, G. E.; Robb, M. A.; Cheeseman, J. R.; Zakrzewski, V. G.; Montgomery, J. A., Jr.; Stratmann, R. E.; Burant, J. C.; Dapprich, S.; Millam, J. M.; Daniels, A. D.; Kudin, K. N.; Strain, M. C.; Farkas, O.; Tomasi, J.; Barone, V.; Cossi, M.; Cammi, R.; Mennucci, B.; Pomelli, C.; Adamo, C.; Clifford, S.; Ochterski, J.; Petersson, G. A.; Ayala, P. Y.; Cui, Q.; Morokuma, K.; Malick, D. K.; Rabuck, A. D.; Raghavachari, K.; Foresman, J. B.; Cioslowski, J.; Ortiz, J. V.; Stefanov, B. B.; Liu, G.; Liashenko, A.; Piskorz, P.; Komaromi, I.; Gomperts, R.; Martin, R. L.; Fox, D. J.; Keith, T.; Al-Laham, M. A.; Peng, C. Y.; Nanayakkara, A.; Gonzalez, C.; Challacombe, M.; Gill, P. M. W.; Johnson, B. G.; Chen, W.; Wong, M. W.; Andres, J. L.; Head-Gordon, M.; Replogle, E. S.; Pople, J. A. *Gaussian 98*, revision A.6; Gaussian, Inc.: Pittsburgh, PA, 1998.
(16) Schmidt, M. W.; Baldridge, K. K.; Boats, J. A.; Elbert, S. T.; Gordon, M. S.; Jensen, J. J.; Koseki, S.; Matsunaga, N.; Nguyen, K. A.; Su, S.; Windus, T. L.; Dupuis, M.; Montgommery, J. A. *J. Comput. Chem.* **1993**, *14*, 1347.
(17) Holland, P. M.; Castleman, A. W. *J. Chem. Phys.* **1981**, *76*, 4195.
(18) Neogrady, P.; Urban, M.; Sadlej, A. J. *J. Mol. Struct. (THEOCHEM)* **1995**, *332*, 197.
(19) *Handbook of Chemistry and Physics*; CRC Press: Boca Raton, 1995.
(20) Henglein, A. *Ber. Bunsen-Ges. Phys. Chem.* **1977**, *81*, 556.
(21) Heller, A.; Reiss, H. *J. Phys. Chem.* **1985**, *89*, 4207.
(22) Krestov, G. A. *Thermodynamics of Solvation*; Ellis Horwood: Chichester, U.K., 1991.
(23) Burgess, J. *Metal Ions in Solution*; Ellis Horwood: Chichester, U.K., 1978.
(24) Tissandier, M. D.; Kowen, K. E.; Feng, W. Y.; Gundlach, E.; Cohen, M. H.; Earhart, A. D.; Coe, J. V. *J. Phys. Chem. A* **1998**, *102*, 9308.
(25) Metropolis, N.; Rosenbluth, A. W.; Rosenbluth, M. N.; Teller, A. H. *J. Chem. Phys.* **1953**, *21*, 1087.
(26) Owicki, J. C.; Scheraga, H. A. *Chem. Phys. Lett.* **1977**, *47*, 600.
(27) Lynden-Bell R. M.; Rasaiah, J. C. *J. Chem. Phys.* **1997**, *107*, 1981.
(28) NBS Technical Note No. 270-4. National Bureau of Standards: Washington, DC, 1968.
(29) Langhoff, S. R.; Pettersson, L. G. M.; Bauschlicher, C. W., Jr.; Partridge, M. *J. Chem. Phys.* **1987**, *86*, 268.